ARTICLE

D1 receptor-expressing neurons in ventral tegmental area alleviate mouse anxiety-like behaviors via glutamatergic projection to lateral septum

Qiuping Tong[1], Xiao Cui[1], Hao Xu[1], Xiaoshuang Zhang[1], Songhui Hu[1], Fang Huang[1] and Lei Xiao[1]✉

Dopamine (DA) acts as a key regulator in controlling emotion, and dysfunction of DA signal has been implicated in the pathophysiology of some psychiatric disorders, including anxiety. Ventral tegmental area (VTA) is one of main regions with DA-producing neurons. VTA DAergic projections in mesolimbic brain regions play a crucial role in regulating anxiety-like behaviors, however, the function of DA signal within VTA in regulating emotion remains unclear. Here, we observe that pharmacological activation/inhibition of VTA D1 receptors will alleviate/aggravate mouse anxiety-like behaviors, and knockdown of VTA D1 receptor expression also exerts anxiogenic effect. With fluorescence in situ hybridization and electrophysiological recording, we find that D1 receptors are functionally expressed in VTA neurons. Silencing/activating VTA D1 neurons bidirectionally modulate mouse anxiety-like behaviors. Furthermore, knocking down D1 receptors in VTA DA and glutamate neurons elevates anxiety-like state, but in GABA neurons has the opposite effect. In addition, we identify the glutamatergic projection from VTA D1 neurons to lateral septum is mainly responsible for the anxiolytic effect induced by activating VTA D1 neurons. Thus, our study not only characterizes the functional expression of D1 receptors in VTA neurons, but also uncovers the pivotal role of DA signal within VTA in mediating anxiety-like behaviors.

Molecular Psychiatry; https://doi.org/10.1038/s41380-022-01809-y

INTRODUCTION

Anxiety disorders are the most common psychiatric diseases, and the prevalence of anxiety disorders is increasing, especially during the COVID-19 pandemic [1]. Deciphering the neural mechanisms underlying anxiety-like behaviors will benefit the treatment of anxiety disorders [2]. Dopamine (DA) is one of the key regulators in mediating emotion. Ventral tegmental area (VTA) is the origin of mesocorticolimbic DA system. Impairment of VTA DA neurons is associated with the development of a persistent, generalized anxiety-like phenotype [3], and direct activation of VTA DA neurons may also trigger anxiety-like behaviors [4]. These seemingly inconsistent findings might be attributable to multiple downstream targets of VTA DA signal. Previous studies have shown that DA released from VTA DA neurons targets multiple mesocorticolimbic brain regions to regulate emotion, including medial prefrontal cortex (mPFC) [5–9], nucleus accumbens (NAc) [7, 8, 10], and amygdala [11, 12]. In addition to releasing DA in mesocorticolimbic regions, VTA DA neurons are also capable to release DA locally within VTA [13, 14], but the involvement of VTA local DA signal in regulating anxiety-like behaviors remains to be identified.

DA regulates neuronal activity to orchestrate brain functions by binding to DA receptors. DA Drd1 (D1) receptor and Drd2 (D2) receptor are two major DA receptors expressed in brain. D1 receptor couples to $G_{\alpha s}$ to activate adenylyl cyclase (AC) and increase cyclic AMP levels, while D2 receptor inhibits AC and calcium channels by coupling to $G_{i/o}$. D2 receptor is the main target for most antipsychotic drugs [15–17]. It is well-known that D2 receptor variants are associated with co-morbid depression and anxiety [18, 19], and dysfunction of D2 receptors in the anterior cingulate cortex and NAc will aggravate anxiety-like behaviors [20, 21]. D1 receptors are associated with cognitive function [22, 23]. D1 receptor in the VTA downstream regions is also found to be involved in regulating depression and anxiety-like behaviors. Activating mPFC D1 receptor-expressing pyramidal neurons produces rapid and long-lasting antidepressant and anxiolytic responses [24]. Stimulation of D1 receptors in dentate gyrus enhances the antidepressant effect of fluoxetine and improves depression-like behaviors [25]. VTA DA signal targets the interpeduncular nucleus to alleviate anxiety-like behaviors via activating D1 receptors [26].

In addition to the downstream brain regions of DA neurons, the expression and possible functions of DA receptors, especially D2 receptors within VTA have been investigated [27–29]. D2 receptors are expressed in the soma, dendrites and axon terminals of VTA DA neurons [30]. The expression of D2 receptors in VTA neurons plays an important role in coordinating locomotion and incentive motivation of psychostimulants [29, 31]. A recent study showed that VTA D2 receptors are the potential target for corticosterone-induced anxiety-like behaviors [32]. In addition to

[1]The State Key Laboratory of Medical Neurobiology, MOE Frontiers Center for Brain Science, and the Institutes of Brain Science, Fudan University, Shanghai 200032, China. ✉email: leixiao@fudan.edu.cn

Received: 11 March 2022 Revised: 18 September 2022 Accepted: 20 September 2022
Published online: 04 October 2022

D2 receptors, previous studies also investigated the functional roles of D1 receptors in VTA, and implicated that blocking D1 receptors impaired excitatory and inhibitory synaptic plasticity [33, 34], and decreased cocaine-induced reward [35] and chemical stimulation-induced anti-nociception [36, 37]. These studies inferred that D1 receptors were expressed in the axonal terminals projecting to VTA neurons. However, the expression of D1 receptors in VTA neurons is still unclear [38–40], and the functional significance of VTA D1 receptors in emotion regulation has not yet been investigated.

To address this gap, we have performed a series of experiments to interrogate the functional expression of D1 receptors in VTA neurons and define the pivotal role of VTA local DA signal in mediating anxiety-like behaviors. We observed that activating/inhibiting VTA D1 receptors will bidirectionally change mouse anxiety level. Utilizing fluorescence in situ hybridization (FISH), combined with transgenic mouse lines and electrophysiological recording, we established the expression of D1 receptors in VTA neurons. We then explored the role and neural circuits of D1 receptor expression in VTA neurons in regulating anxiety-like behaviors with a combination of optogenetics, chemogenetics, pharmacological tools, and RNA interference. Our results uncover the significance of DA signal within VTA in mediating anxiety-like behaviors.

MATERIALS AND METHODS

Mice

Mice were handled following the protocols approved by the Fudan University Animal Care and Use Committee. Six to ten weeks old male and female animals were used in this study. Following mouse lines were used: C57BL/6, D1-Cre (034258-UCD, MMRRC), DAT-Cre (#006660, Jackson Laboratory), Vglut2-Cre (#016963, Jackson Laboratory), and Vgat-Cre (#017535, Jackson Laboratory) mice. Genotyping were conducted following standard procedures on the Jackson Lab or MMRRC websites.

Short-hairpin RNA and virus preparation

DA Drd1 receptor short-hairpin RNA sequence (5′AAGAGCATATGCC ACTTTGTATT3′) was chosen according to previous published works [41, 42]. Sequences encoding shRNA were inserted into rAAV-U6-CMV-EGFP-pA or rAAV-CMV-DIO-(EGFP-U6) -WPRE-hGH-pA vectors. Adeno-associated virus 9 (AAV9) expressing Drd1 RNAi (5.0×10^{12} vector genomes/mL and 5.07×10^{12} vector genomes/mL for non-Cre and Cre-dependent viruses) or control RNAi (5.7×10^{12} vector genomes/mL and 5.66×10^{12} vector genomes/mL for non-Cre and Cre-dependent control viruses) were packaged by BrainVTA Technology Co, Ltd (Wuhan, China). The efficiency of the Drd1 siRNA construct was tested after behaviors with qRT-PCR analysis using the tissue samples collected from VTA.

In vivo stereotaxic intracranial injection

Mice aged 4–7 weeks were anesthetized with 1–2% isoflurane, and placed in a stereotaxic apparatus (E07370-005, RWD). Recombinant AAVs were delivered into brain regions by a microsyringe pump controller (NanoJect III, Drummond Scientific Company). Animals recovered for at least three weeks after surgery.

Optical fiber and cannula implantation

For in vivo photostimulation experiments, an optical fiber (200 μm, 0.37 NA, Newdoon) was implanted into the related brain region. For local drug microinjection, mice were implanted with a stainless-steel guide cannula (26-gauge) above VTA or LS. At least 1 week after surgery, mice were used for behavioral tests. Brains were sectioned to verify fiber or cannula location after behavioral tests. Mice with incorrect implantation locations were excluded from analyses. Detailed information were summarized in Supplementary Table 1.

Acute slice preparation and electrophysiological recording

Acute brain slices were prepared from mice as previously described [43–45]. Neurons were visualized in slices using an IR/DIC microscopy. Recordings were made using 700B amplifier, data were digitized at 10 kHz and filtered at 4 kHz and collected using pCLAMP software (Molecular Devices).

Tissue processing, immunohistochemistry, and imaging

Animals were anesthetized with isoflurane, and perfused with 4% paraformaldehyde (PFA). Sliced tissues were chosen and pretreated in 0.2% Triton-X100 for 1 h at room temperature (RT), then blocked with 0.05% Triton-X100, 10% bovine serum albumin (BSA) in PBS for 1 h at RT and rinsed in PBS. Tissues were transferred into primary antibody solution for 24 h at 4 °C. After incubating with secondary antibody solution, slices were mounted onto glass slides, and imaged with an Olympus VS120 slide scanning microscope.

Quantitative fluorescence single molecule in situ hybridization (smFISH)

smFISH was conducted following previously published procedures [43, 44]. Following probes were used in this study: *Slc17a6* (*Vglut2*, C1, 318171), *Slc32a1* (*Vgat*, C1, 319191), *Drd1a* (C2, 406491), *Th* (Tyrosine hydroxylase, C3, 317621), *EYFP* (C3, 312131). Probe omission negative controls were carried out for every reaction.

mRNA quantification

Tissues were homogenized and total RNA was isolated using Trizol reagent (TianGen, China) according to the manufacturer's instruction and kept at −80 °C before use. Murine β-actin was used as a reference to normalize the targeted gene expression levels.

Behavior assays. Behavioral tests were conducted between 1:00–9:00 pm. Mice were habituated in behavior room for at least 1 h before beginning the experimental testing. If not specifically stated, behavioral tests were performed with light off. Behavioral apparatuses were cleaned and wiped with 70% ethanol to remove odor clues left by the previous subject between trials. Mouse trajectories were detected with Toxtrac software (https://toxtrac.sourceforge.io), then analyzed with self-written MATLAB scripts.

Statistical analyses. In our study, no statistical method was used to predetermine sample sizes, and the sample sizes were determined based on previous studies conducted in the same field. Normality was assessed by the Shapiro-Wilk test. For normal distributions, homoscedasticity was assessed by *F*-test using GraphPad Prism. For homogeneous variances, two-tailed *t*-test and paired/unpaired *t*-test were used for single and paired comparisons, and one-way ANOVA followed by *post hoc* Tukey's test was used for multiple comparisons. When variances were not homogeneous, a *t*-test with Welch's correction was used. For data that were not normally distributed, Wilcoxon signed rank test, Mann-Whitney test or Wilcoxon matched-pairs signed rank test was used for single and paired comparisons, and Friedman test followed by *post hoc* Dunn's test was used for multiple comparisons. Detailed statistical information and *p* value for every data set were summarized in Supplementary Table 2.

More details on experimental procedures can be found in the Supplementary Information.

RESULTS

Manipulating VTA D1 receptors bidirectionally regulates mouse anxiety-like behaviors

With a cannula unilaterally implanted into the VTA of male and female mice, we explored the effect of activating/inhibiting D1 receptors on mouse anxiety-like behaviors via microinjecting D1 receptor agonist (A68930)/antagonist (SCH23390) (Fig. 1A). Mouse anxiety-like behaviors were evaluated with open-field test and elevated plus maze (EPM) test [2]. Activating D1 receptors had no effect on mouse locomotion, but increased the time spent at center region in open-field test in both male and female (Fig. 1B, D, E). Consistent with open-field test, D1 agonist increased the time spent at open arms in EPM test (Fig. 1B, F), but did not change the frequency entering open arms (Supplementary Fig. 1A). On the contrary, inhibiting VTA D1 receptors induced anxiety-like behaviors, as indicated by decreased time exploring

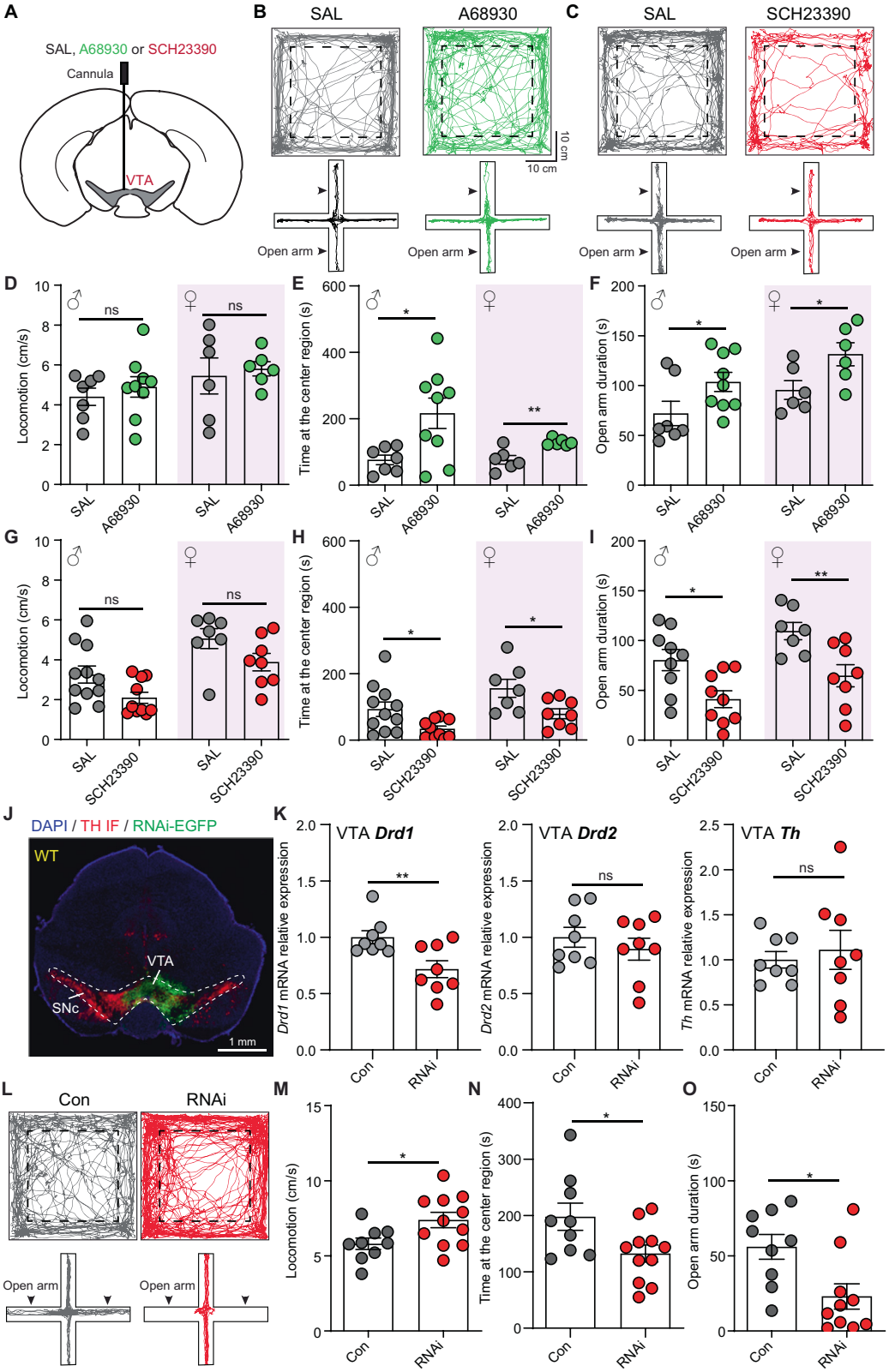

center region in open-field test and open arms in EPM test (Fig. 1C, G–I). However, manipulating VTA D1 receptors had no significant effect on social motivation and social exploration (Supplementary Fig. 1A, B). These results suggest that activating/inhibiting VTA D1 receptors bidirectionally regulate mouse anxiety-like behaviors.

We then evaluated the effect of reducing D1 receptor expression in VTA neurons on anxiety-like behaviors. D1 receptors were knocked down by using RNA interference (RNAi) [41, 42]. The efficiency of RNAi in reducing VTA *Drd1* expression was validated by quantitative PCR, and VTA *Drd1* mRNA was reduced to be about 70% (71.71 ± 7.5%), but *Drd2* and *Th* mRNA levels were not changed

Fig. 1 Manipulating VTA D1 receptors bidirectionally regulates mouse anxiety-like behaviors. A Schematic illustration of pharmacological experiment. D1 receptor agonist A68930, D1 receptor antagonist SCH23390, or saline (SAL) were unilaterally injected into the VTA. **B** Example trajectories of mice with SAL (Left) and A68930 (Right) treatment in open-field test (Top) and EPM test (Bottom). Dashed boxes indicate the center region. **C** Same as **B**, but for mice with SAL and SCH23390 microinjection. **D** Summary of mouse locomotor speed with microinjection of SAL and A68930 into the VTA. $n = 7$ male mice and 6 female mice for SAL groups, and 9 male mice and 6 female mice for A68930 groups, Unpaired *t*-test test. **E** and **F** Same as **D**, but for the time spent at the center region (**E**), and the time spent at the open arms in EPM test (**F**). $^{*}p < 0.05$, $^{**}p < 0.01$, Mann–Whitney test for male open arm duration in EPM test, and Unpaired *t*-test for other comparisons. **G–I** Same as **D–F**, but for microinjecting SAL and SCH23390 into the VTA. $n = 11$ male mice and 7 female mice for SAL groups, and 10 male mice and 8 female mice for SCH23390 groups in open-field test; $n = 9$ male mice and 7 female mice for SAL groups, and 9 male mice and 8 female mice for SCH23390 groups in EPM test, $^{*}p < 0.05$, $^{**}p < 0.01$, Mann–Whitney test for locomotion in open-field test, and Unpaired *t*-test for other comparisons. **J** An example image showing AAV9-U6-shRNA(Drd1)-EGFP virus expression in VTA. TH IF: red. **K** Relative VTA *Drd1*, *Drd2*, and *Th* mRNA expression in control mice ($n = 8$) and RNAi mice ($n = 8$). $^{**}p < 0.01$, Unpaired *t*-test. **L** Example trajectories in open-field test (Top) and EPM test (Bottom) for one control (Con) mouse (Left) and one RNAi mouse (Right). **M** Locomotor speed of Con and RNAi mice. $^{*}p < 0.05$, Unpaired *t*-test, $n = 9$ and 11 male mice for control and RNAi mice, respectively. **N** and **O** Same as **M**, but for the time spent at the center region in open-field test (**N**) and time spent at the open arms in EPM test (**O**).

(Fig. 1J–K). In open-field test, reducing D1 receptor increased mouse locomotor speed and decreased the time spent at center region in both male and female (Fig. 1L–N; Supplementary Fig. 1C). In EPM test, the duration spent at open arms was significantly decreased after lowering D1 receptors (Fig. 1L, O; Supplementary Fig. 1C). Reducing VTA D1 receptor had no effect on social exploration (Supplementary Fig. 1D–E). Therefore, VTA D1 receptor is involved in relieving anxiety-like behaviors.

D1 receptors are functionally expressed in VTA neurons

Since D1 receptor expression in VTA neurons remains unclear, we explored the expression of D1 receptors in VTA with quantitative fluorescence in situ hybridization (FISH). Different from the extensive expression of *Drd2* in VTA DA neurons [29], *Drd1* mRNA was sparely expressed (Supplementary Fig. 2A). In addition to DA neurons, VTA also contains GABA and glutamate neurons [46]. The co-localization of *Drd1* with *Slc32a1* (*Vgat*), *Slc17a6* (*Vglut2*), and *Th* (Tyrosine hydroxylase) were analyzed (Fig. 2A, B). The composition of $Drd1^{+}$ neurons in VTA includes ~48.8% Th^{+}, ~24.4% $Vgat^{+}$, and ~43.1% $Vglut2^{+}$ neurons. VTA DA neurons are capable to co-release glutamate and GABA [46–48], so we further analyzed the co-localization of $Drd1^{+}$, Th^{+} neurons with glutamate and GABA neurons, and found that ~68.1% of $Drd1^{+}$, Th^{+} neurons are $Vglut2^{+}$, but very few are $Vgat^{+}$ (~8.7%) (Fig. 2B). Meanwhile, compared with a high proportion of VTA DA neurons expressing *Drd2*, ~20% of Th^{+} neurons co-localize with *Drd1* probes (24.0 ± 5.8%, 5761 Th^{+} neurons from 5 mice), ~20% of $Vglut2^{+}$ neurons express *Drd1* mRNA (20.34 ± 3.1%, 1036 $Vglut2^{+}$ neurons from 2 mice), and only ~10% of $Vgat^{+}$ neurons express *Drd1* mRNA (10.33 ± 0.2%, 2193 $Vgat^{+}$ neurons from 2 mice). *Drd1* expression in VTA DA neurons is sex invariant, with 21.8 ± 7.9% and 27.2 ± 11.5% VTA Th^{+} neurons co-localize with *Drd1* for male and female mice (3 male and 2 female).

With the D1-Cre mouse line [49], we confirmed the expression of D1 receptors in VTA neurons. To assess the fidelity of D1-Cre mouse line, AAV9-DIO-eYFP viruses were injected into VTA to label Cre-positive neurons (Fig. 2C). We observed that *Drd1* was present in ~75% of $eYFP^{+}$ neurons (267 $Drd1^{+}$/357 eYFP VTA neurons from 2 mice, Fig. 2C, D). ~39.7% (739/1862 $eYFP^{+}$ neurons from 2 mice) eYFP labeled neurons were colocalized with TH^{+} neurons (Supplementary Fig. 2B), in line with the FISH results (Fig. 2B). We then explored the effect of activating D1 receptors on VTA neurons. With intraperitoneal injection of A68930 (5 mg/kg), ~40% $eYFP^{+}$ neurons in VTA were activated, immunolabeled via cFos staining, but very few (~4.5%) after saline injection (Fig. 2E). Using in vitro patch-clamp technique, 1 μM A68930 application significantly increased the activity of VTA $eYFP^{+}$ neurons (Fig. 2F, G).

We also investigated whether endogenous VTA DA release was sufficient to activate D1 receptors in VTA neurons. A small volume of AAV9-DIO-ChR2-mCherry viruses were injected into the VTA of DAT-Cre mice to infect DA neurons (Fig. 2H). As mentioned, VTA DA neurons co-release GABA and glutamate [46–48], and local DA release can activate D2 receptors, so cocktail drugs were used to block GABA(A), GABA(B), AMPA, NMDA, and D2 receptors during the experiment. Blue light pulses (10-ms long, 100 pulses) at 5 Hz, 10 Hz, and 20 Hz reliably excited VTA mCherry-positive neurons (Supplementary Fig. 2C). Firing rates of some VTA mCherry-negative neurons, recorded in cell-attached voltage-clamp mode, were increased when the light stimulation was given, especially at 10 and 20 Hz (Fig. 2I, J). Light-responsive neurons were defined as those exhibiting at least a 15% change of firing rate relative to baseline during light stimulation. The proportion of VTA mCherry-negative neurons excited by light stimulation was increased with optical stimulation frequency, and about 25% (5/20 neurons from 7 mice), 35% (7/20 neurons), and 50% (10/20 neurons) neurons were excited by optical stimulation at 5 Hz, 10 Hz, and 20 Hz, respectively (Supplementary Fig. 2D). To confirm the involvement of D1 receptors in light-induced firing rate increase, D1 receptor antagonist SCH23390 was added into the perfusion solution, and the degree of light-induced firing rate increase of VTA mCherry-negative neurons was significantly blocked (Fig. 2K and Supplementary Fig. 2E).

Activating/silencing VTA D1 neurons oppositely modulate mouse anxiety-like behaviors

Both FISH and electrophysiological results provided compelling evidence of that D1 receptors are functionally expressed in VTA neurons (Fig. 2). Since manipulating VTA D1 receptors changed mouse anxiety-like behaviors (Fig. 1), we explored the role of VTA D1 neurons in regulating anxiety. AAV9-DIO-ChR2-mCherry viruses were injected into VTA of D1-Cre mice to optically manipulate D1 neurons (Fig. 3A). VTA $ChR2^{+}$ neurons reliably responded to the 10-ms long blue light pulses with frequency at 10 Hz and 20 Hz (Fig. 3B). Time spent at center region in open-field test was significantly increased when stimulating with 20 Hz, but not 1 Hz or 10 Hz light pulses in both male and female (Fig. 3C, E; Supplementary Fig. 3G, H). Optical activating VTA D1 neurons with 10 and 20 Hz, but not 1 Hz light pulses, increased mouse locomotor speed (Fig. 3C, D; Supplementary Fig. 3G, H). Further analyses showed that activating VTA D1 neurons only increased the locomotor speed at surround region, but not at center region (Fig. 3F). The ratio between center and surround locomotor speeds was significantly reduced with optical stimulation at 20 Hz, but not changed at 1 Hz or 10 Hz (Fig. 3F and Supplementary Fig. 3E). The locomotion and time spent at center region in open-field test did not change with light stimulation for mice with only mCherry virus expression (Supplementary Fig. 3A–E).

We also validated the anxiolytic effect of activating VTA D1 neurons by EPM test. Activating VTA D1 neurons with 20 Hz light stimulation did not change the frequency entering open arms, but significantly increased the duration spent at open arms (Fig. 3G, H; Supplementary Fig. 3F). Activating VTA D1 neurons induced anxiolytic effect was consistent in both male and female (Supplementary Fig. 3I). Similar as microinjection of D1 receptor

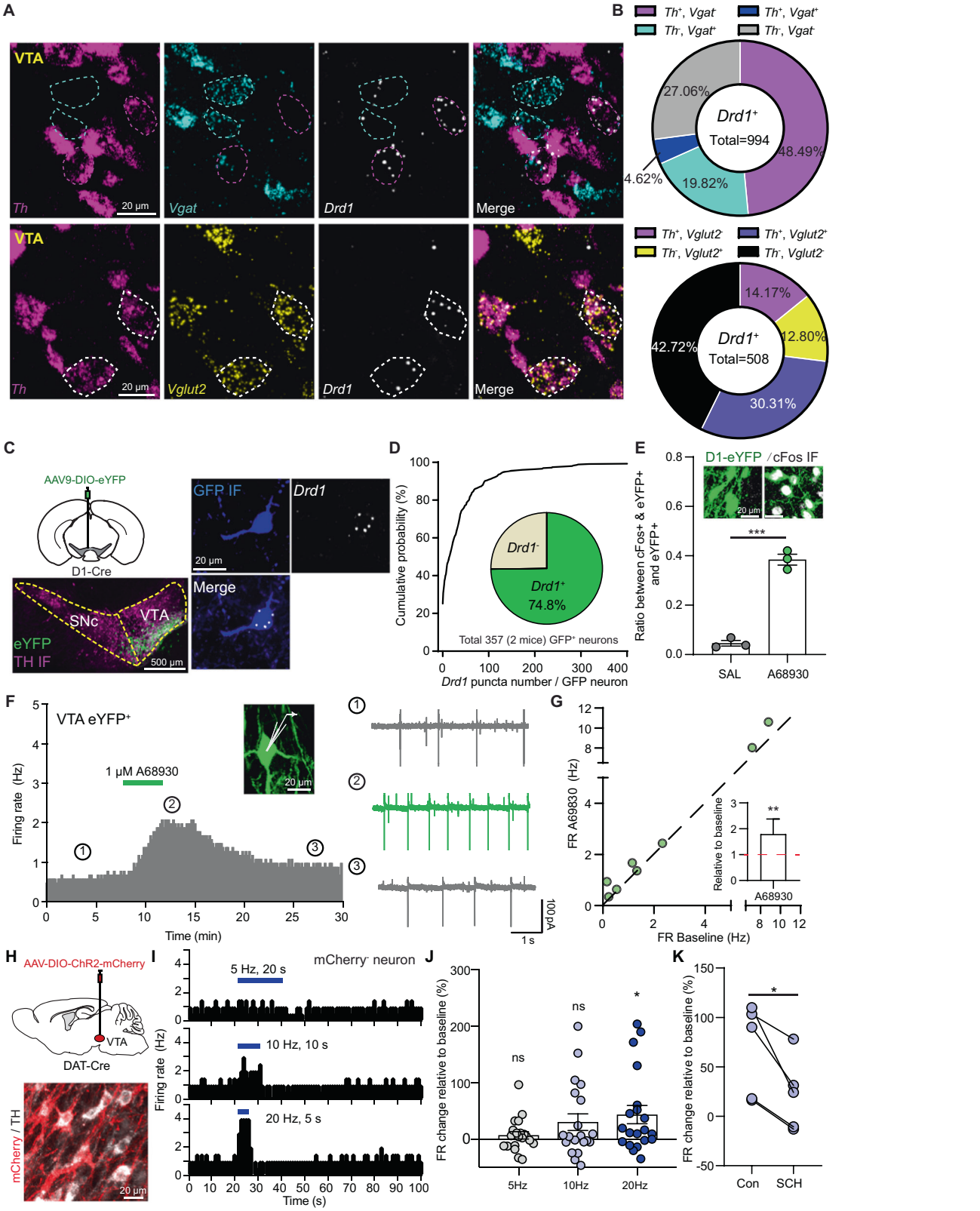

agonist, no effect on social exploration was observed when activating VTA D1 neurons (Supplementary Fig. 3J–L).

We further utilized chemogenetic approach to corroborate the role of VTA D1 neurons in regulating anxiety-like behaviors. AAV viruses with hM3Dq-mCherry, hM4Di-mCherry, or mCherry were expressed into VTA D1 neurons (Fig. 4A). Intraperitoneal injection of clozapine-n-oxide (CNO, 2 mg/kg) increased cFos expression in hM3Dq-mCherry neurons, but not in hM4Di-mCherry neurons (Fig. 4B and Supplementary Fig. 4A, B). In cell-attached recording, 5 μM CNO application increased and decreased the activities of VTA D1 neurons expressing hM3Dq and hM4Di, respectively (Fig. 4B). Consistent with optical activation, chemogenetic activation of VTA

Fig. 2 Functional expression of D1 receptors in VTA neurons. A Fluorescence in situ hybridization (FISH) images in VTA with *Th*, *Vgat*, and *Drd1* probes (Top), and with *Th*, *Vglut2*, and *Drd1* probes (Bottom). *Th* (magenta), vesicular GABA transporter (*Slc32a1/Vgat*, cyan), vesicular glutamate transporter 2 (*Slc17a6/Vglut2*, yellow) and *Drd1* (white). The dashed circles indicate $Drd1^+$ neurons, and magenta indicates Th^+, cyan indicates $Vgat^+$, and white indicates both Th^+ and $Vglut2^+$. **B** Quantitative analyses of *Th*, *Vgat*, and *Drd1* co-expression (Top, 994 $Drd1^+$ neurons from 1 male and 1 female mice), and *Th*, *Vglut2*, and *Drd1* co-expression (Bottom, 508 $Drd1^+$ neurons from 1 male and 1 female mice). **C** Left top: schematic of viral transduction strategy to express eYFP in VTA Cre^+ neurons of D1-Cre mice. Left bottom: an example image showing eYFP expression in VTA. TH IF: magenta. Right: a confocal image showing co-localization of $eYFP^+$ neuron (GFP IF, blue) and *Drd1* mRNA puncta (white). **D** Cumulative probability of $Drd1^+$ puncta in VTA GFP neurons. Insert: quantification of the co-localization of GFP IF positive neurons and *Drd1* mRNA. $n = 357$ GFP^+ neurons from 2 female mice. **E** Ratio of VTA $eYFP^+$ neurons colocalized with cFos signal for D1-Cre mice with saline (SAL) and A68930 intraperitoneal injection. $^{***}p < 0.001$, Unpaired *t*-test, $n = 3$ (2 female and 1 male) mice for the SAL and A68930 injection, respectively. Inset images showing co-localization of $eYFP^+$ neuron (Green) and cFos signal (white) for D1-Cre mice with saline (SAL, left) or A68930 (right) injection. **F** Left: firing rate histogram (10 s bins) from a VTA eYFP labeled neuron with application of 1 μM A68930. Right: example traces correspond to time points 1–3 as shown in the Left panel. **G** Firing rates (FR) of VTA $eYFP^+$ neurons before and during A68930 application. Inset: FR with A68930 application of VTA $eYFP^+$ neurons relative to baseline. $^{**}p < 0.01$, Wilcoxon signed rank test, $n = 8$ neurons from 5 mice. **H** Expression of ChR2-mCherry in VTA DAT^+ neurons. **I** FR histogram (1 s bins) from a VTA mCherry-negative neuron with blue light stimulation at 5 Hz (Top), 10 Hz (Middle), and 20 Hz (Bottom). Blue bars indicate light stimulation. **J** Summary of light-induced firing rate change of VTA mCherry-negative neurons. Wilcoxon signed rank test, $^{*}p < 0.05$, $n = 20$ neurons from 7 (3 male and 4 female) mice. **K** FR change of VTA mCherry-negative neurons in response to light stimulation at 10 Hz before and during the application of D1 receptor antagonist (10 μM SCH23390). $^{*}p < 0.05$, Paired *t*-test, $n = 5$ neurons from 5 (2 male and 3 female) mice.

D1 neurons significantly increased the time spent at center region in open-field test, and chemogenetic inhibition reduced time spent at center region (Fig. 4C, E). Unexpectedly, both chemogenetic activation and inhibition increased mouse locomotor speed (Fig. 4C, D). Further analyses showed that chemogenetic activation and inhibition both increased the locomotor speed at surround region, while the center locomotor speed was only increased when chemogenetic inhibiting D1 neurons (Supplementary Fig. 4C, D). Consistent with optogenetic activating VTA D1 neurons, the ratio between center and surround locomotor speeds was reduced when chemogenetic activating D1 neurons, but not changed when inhibiting D1 neurons (Fig. 4F). We speculate that though activating/inhibiting VTA D1 neurons both increased locomotor speed, locomotion increased by activating D1 neurons may promote environment exploration related with less anxiety whereas locomotion increase induced by inhibiting D1 neurons may be an anxiety-like phenotype [50]. For the mice transduced with only mCherry viruses, CNO had no effect on mouse behavior in open-field test (Fig. 4C–E, Supplementary Fig. 4C, D). However, chemogenetic manipulating VTA D1 neurons had no obvious effect on open arm duration in EPM test (Supplementary Fig. 4E), which may due to the repeated EPM tests for every mice [51]. Social exploration was also not changed by chemogenetic manipulation (Supplementary Fig. 4F).

To confirm the anxiety-like behavior change induced by inhibiting VTA D1 neurons, we expressed tetanus toxin (TetTox) into VTA D1 neurons (Fig. 4G), which will block synaptic transmission and may have a similar effect as inhibiting neurons [52]. Compared with the control mice, TetTox expression increased mouse locomotor speed, decreased time spent at the center region in open-field test, and had no effect on the center locomotor speed/surround speed ratio (Fig. 4H–J, Supplementary Fig. 4G, J). But mice with TetTox injection spent more time at open arms in EPM test (Supplementary Fig. 4H, J), which may due to the different effect of TetTox on DA release (see "Discussion") [53–55]. TetTox expression had no effect on social interaction (Supplementary Fig. 4I). Together, these results further corroborate that manipulating VTA D1 neuronal activity will modulate mouse anxiety-like behaviors.

Reducing D1 receptors in VTA DA and glutamate neurons increases anxiety-like behaviors, and in GABA neurons alleviates anxiety

Since VTA consists of DA, GABA, and glutamate neurons [46] and D1 receptor mRNA has been detected in all of these types (Fig. 2), we investigated the role of D1 receptor expression in different VTA neurons in regulating anxiety-like behaviors. Firstly, the roles of different neurons in anxiety-like behaviors were separately studied with expressing ChR2 into VTA DA, GABA, or glutamate neurons, and optical fiber was implanted into VTA (Fig. 5A and Supplementary Fig. 5A). The 20 Hz optical stimulation same as used to activate VTA D1 neurons was utilized [56–59]. Activating DA neurons and GABA neurons oppositely changed mouse locomotor activity, but activating glutamate neurons had no effect (Fig. 5B and Supplementary Fig. 5B). Time spent at center region was significantly increased when activating DA neurons and glutamate neurons, but not GABA neurons (Fig. 5C). Though activating DA and GABA neurons changed mouse locomotor speed, the ratio between center and surround speeds was not changed after activation (Fig. 5D). In EPM test, activating glutamate neurons, but not DA or GABA neurons, significantly increased the duration spent at open arms (Fig. 5E, F). Thus, activating VTA glutamate neurons will consistently alleviate mouse anxiety-like behaviors.

In order to study the involvement of D1 receptor expression in VTA different neurons in regulating anxiety-like behaviors, Cre-dependent RNAi viruses were delivered into the VTA of DAT-Cre, Vgat-Cre, and Vglut2-Cre mice, respectively (Fig. 5G). Mouse locomotor speed was significantly increased after reducing D1 receptor expression in VTA DA neurons, but not changed in GABA or glutamate neurons (Fig. 5H, I). Lowering D1 receptors in VTA DA neurons had no effect on the time spent at center region in open-field test, but in GABA neurons increased the center staying time and in glutamate neurons decreased the duration (Fig. 5J). Reducing D1 receptor expression in DA neurons tended to increase locomotor speed at both center and surround regions (Supplementary Fig. 5C, D), but the ratio between center and surround speeds decreased after lowering D1 receptors in GABA neurons, but not in DA or glutamate neurons (Fig. 5K). In EPM test, the duration spent at open arms was slightly reduced after lowering D1 receptors in DA neurons and glutamate neurons, but not in GABA neurons (Fig. 5L). The frequency entering open arms and social related behaviors did not change after lowering D1 receptors (Supplementary Fig. 5E, F). Together, these results suggest that lowering D1 receptors in DA and glutamate neurons exerts anxiogenic effect, while reducing D1 receptor expression in GABA neurons will be anxiolytic.

Glutamategric projection of VTA D1 neurons to lateral septum alleviates mouse anxiety-like behaviors

VTA neurons project to many brain regions, including NAc, mPFC, lateral septum (LS), basolateral amygdala (BLA), ventral hippocampus (vHipp) to regulate emotional behaviors [60–63]. With AAV-DIO-eYFP injected into the VTA of D1-Cre mice, we observed the distributions of D1 neuronal axons in mPFC, NAc, LS, BLA, and vHipp (Fig. 6A and Supplementary Fig. 6A), which suggested that

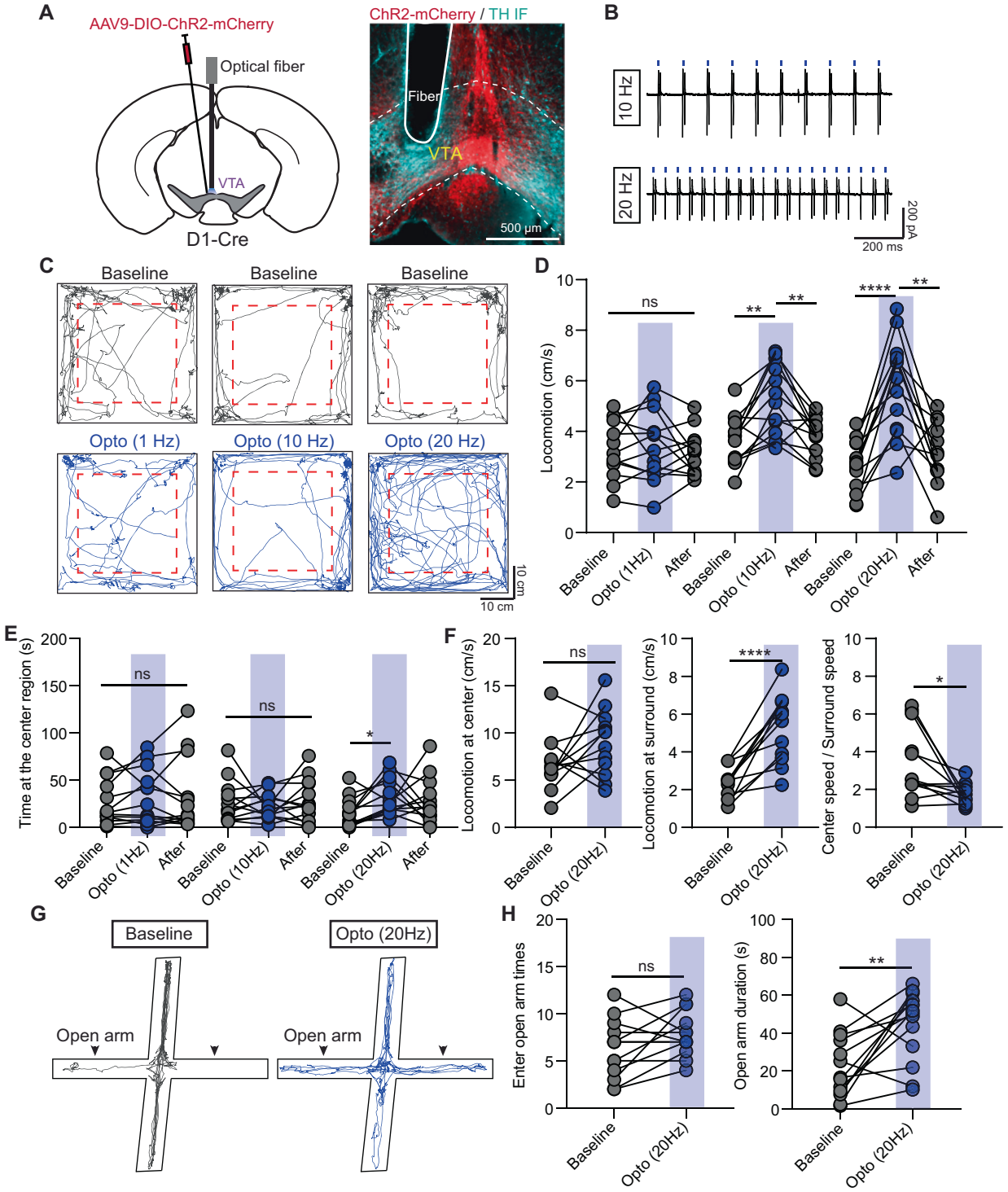

Fig. 3 Optogenetic activation of VTA D1 neurons relieves mouse anxiety-like behaviors. A Left: Schematic of viral transduction strategy to express ChR2-mCherry in VTA D1 neurons. Right: an example image showing the ChR2-mCherry expression and the location of implanted optical fiber. ChR2-mCherry: red; TH IF: cyan. **B** Cell-attached recording traces of a VTA ChR2-mCherry^{+} neuron in response to 10-ms-long 470 nm light pulses at 10 Hz (Top) and 20 Hz (Bottom). **C** Trajectories of one mouse in open-field test before (Top) and during light stimulation (Bottom) with frequency at 1 Hz (Left), 10 Hz (Middle), and 20 Hz (Right). Dashed boxes indicate the center region. **D** Statistical results of locomotor speed before, during, and after 5-min light stimulation with frequency at 1 Hz, 10 Hz, and 20 Hz, respectively. One-way ANOVA with Tukey's multiple comparisons *post hoc* test, $n = 13$ (9 male and 4 female) mice, $^{**}p < 0.01$, $^{****}p < 0.0001$. **E** Same as **D**, but for time spent at the center region. $^{*}p < 0.05$, One-way ANOVA with Tukey's multiple comparisons *post hoc* test. **F** Statistical results of the locomotor speed at the center region (Left), locomotor speed at the surround region (middle), and ratio between locomotor speed at center and surround regions before and during light stimulation with frequency at 20 Hz. $n = 12$ (8 male and 4 female) mice, $^{*}p < 0.05$, $^{****}p < 0.0001$, Paired *t*-test for the surround locomotion and Wilcoxon matched-pairs signed rank test for the ratio between center and surround speeds. **G** Trajectories of one mouse in EPM test without (Left) and with (Right) light stimulation at 20 Hz. **H** Statistical results of times entering the open arms (Left) and the duration staying at the open arms (Right) without and with light stimulation at 20 Hz, respectively. $n = 13$ mice, $^{**}p < 0.01$, Paired *t*-test.

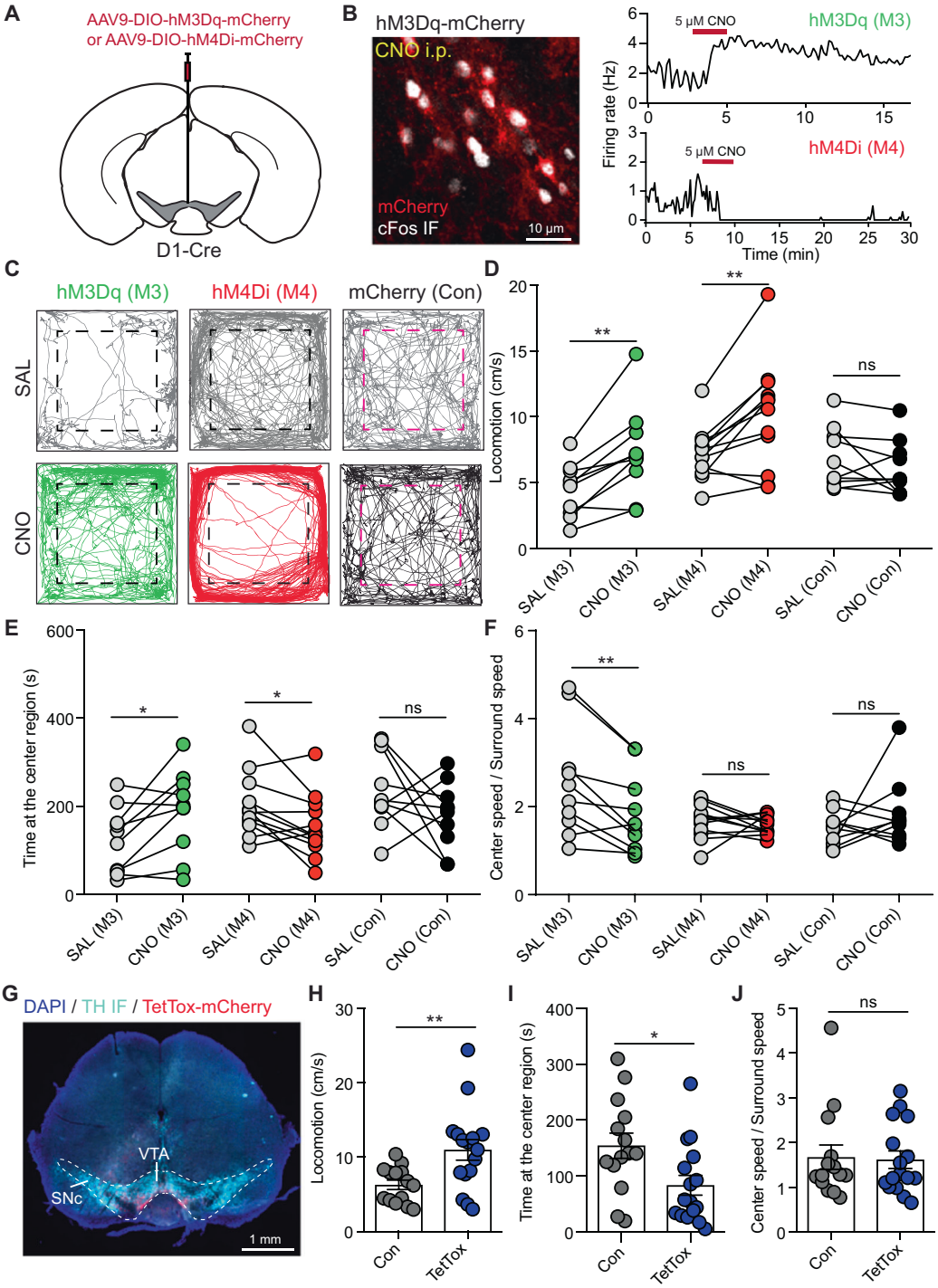

Fig. 4 Chemogenetic manipulation of VTA D1 neurons and blocking synaptic transmission of VTA D1 neurons change mouse anxiety-like behaviors. A Schematic of viral transduction strategy to specifically express hM3Dq-mCherry or hM4Di-mCherry in VTA D1 neurons. **B** Left: intraperitoneal injection (2 mg/kg) of CNO increased cFos expression (white) in VTA hM3Dq-mCherry-positive neurons. Right: bath application of 5 μM CNO increased and decreased the firing rate of hM3Dq-mCherry (Top) and hM4Di-mCherry (Bottom) positive neurons, respectively. **C** Left: trajectories of one mouse in open-field test with hM3Dq-mCherry expression in VTA D1 neurons with saline (Top) and CNO (Bottom) intraperitoneal injection (2 mg/kg). Middle and Right: same as (Left), but with hM4Di-mCherry and mCherry expression in VTA D1 neurons. Dashed boxes indicate the center region. **D** Locomotor speed for mice with hM3Dq, hM4Di or mCherry expression in VTA D1 neurons after saline (SAL) or CNO injection in open-field test. $n = 10$ (7 male and 3 female), 12 (7 male and 5 female), and 10 (5 male and 5 female) mice for hM3Dq (M3), hM4Di (M4), and mCherry (Con) groups. Paired t-test, $^{**}p < 0.01$. **E** Same as **D**, but for the time spent at the center region. Paired t-test, $^{*}p < 0.05$. **F** The ratio between center speed and surround speed in open-field test for mice with hM3Dq, hM4Di, and mCherry expression in VTA D1 neurons after saline (SAL) or CNO injection. Paired t-test, $^{**}p < 0.01$. **G** Example image showing TetTox-mCherry expression in VTA of one D1-Cre mouse. TetTox-mCherry: red; TH IF: cyan. **H** Locomotor speed of mice with mCherry (Con) and TetTox-mCherry (TetTox) expression in VTA D1 neurons. Unpaired t-test, $^{**}p < 0.01$, $n = 14$ (6 male and 8 female) and 16 (7 male and 9 female) mice for Con and TetTox groups, respectively. **I** and **J** Same as **H** but for the time spent at the center region (I), and the ratio between center speed and surround speed in open-field test (**J**). Mann-Whitney test, $^{*}p < 0.05$.

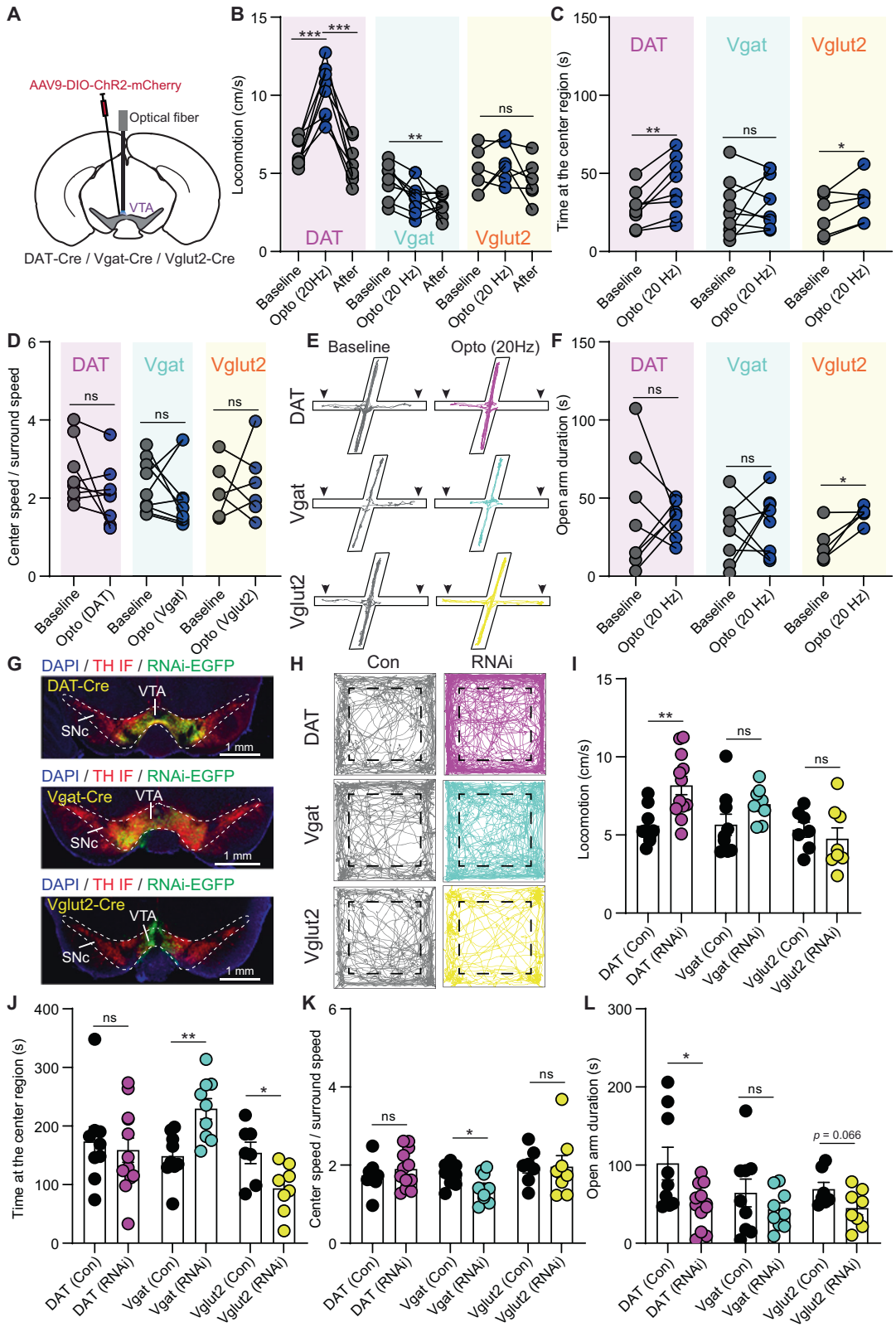

VTA D1 neurons may target these brain regions to regulate anxiety-like behaviors. To define the possible target(s) of VTA D1 neurons involved in regulating anxiety, ChR2-mCherry viruses were expressed into D1 neurons and optical fiber was unilaterally implanted into the mPFC, NAc, LS, BLA, or vHipp (Fig. 6B and Supplementary Fig. 6B, C). For the mice with fiber implanted into mPFC, NAc, BLA or vHipp, light stimulation at 20 Hz had no significant effects on locomotor speed and time spent at center region in open-field test, or time spent at open arms in EPM test (Supplementary Fig. 6D–G). Surprisingly, activating D1 neuronal

Fig. 5 Lowering D1 receptor expression in VTA DA, GABA, and glutamate neurons differently changes mouse anxiety-like behaviors. **A** Schematic of viral transduction strategy to express ChR2-mCherry in VTA DA, GABA, and glutamate neurons and optical fiber targeting the VTA. **B** Statistical results of locomotor speed before, during, and after 5-min light activation of VTA DA, GABA, and glutamate neurons with light stimulation frequency at 20 Hz. $n = 8$ (1 male and 7 female), 9 (6 male and 3 female), and 6 (3 male and 3 female) mice for DAT-Cre, Vgat-Cre, and Vglut2-Cre groups, respectively. $^{**}p < 0.01$, $^{***}p < 0.001$, One-way ANOVA with Tukey's multiple comparisons *post hoc* test. **C** and **D** Same as **B**, but for the time spent at the center region (**C**) and the ratio between speed at the center and surround regions (**D**) in open-field test. $^{*}p < 0.05$, $^{**}p < 0.01$, Paired *t*-test. **E** Trajectories in EPM test with and without optically activating VTA DA, GABA and glutamate neurons. Arrows indicate the open arm side. **F** Statistical results of duration spent at open arms in EPM test with and without optical stimulation to activating VTA DA, GABA, and glutamate neurons. * $p < 0.05$, Paired *t*-test. **G** Example images showing AAV9-CMV-DIO-(EGFP-U6)-shRNA(Drd1) virus expression in VTA of DAT-Cre (Top), Vgat-Cre (Middle) and Vglut2-Cre (Bottom) mice. **H** Trajectories in open-field test for control mice (Left, Con) and the mice with lowering D1 receptors in VTA DA, GABA, and glutamate neurons (Right, RNAi), respectively. Dashed boxes indicate the center region. **I** Locomotor speed of control (4 male and 5 female) and RNAi (5 male and 7 female) DAT-Cre mice, control (9 male) and RNAi (9 male) Vgat-Cre mice, and control (4 male and 3 female) and RNAi (5 male and 3 female) Vglut2-Cre mice. $^{**}p < 0.01$, Unpaired *t*-test. **J**, **K** Same as **I**, but for the time spent at the center region (**J**) and the ratio between center locomotor speed and surround locomotor speed in open-field test (**K**). $^{*}p < 0.05$, $^{**}p < 0.01$, Unpaired *t*-test. **L** Duration spent at open arms in EPM test for control and RNAi in different types of VTA neurons. $^{*}p < 0.05$, Unpaired *t*-test.

axons in LS increased locomotor speed and time spent at center region in open-field test, and also decreased the ratio between center and surround speeds (Fig. 6C, D). Meanwhile, light stimulation in LS significantly increased the duration spent at open arms in EPM test (Fig. 6E). These results suggest that LS is the potential target of VTA D1 neurons to alleviate anxiety-like behaviors.

We then investigated the effect of activating VTA D1 neurons on LS neuronal activity. cFos expressions in VTA and LS were increased with optically activating VTA D1 neurons (Fig. 6F). Synaptic connection between VTA D1 neurons and LS neurons was further examined, and postsynaptic currents in LS neurons were recorded when optically activating VTA D1 neuronal axons (Fig. 6G). Light-evoked postsynaptic current was observed in ~40% LS neurons when membrane voltage was held at −70 mV (15/36 neurons from 7 mice), but no response was detected when held at 0 mV (Fig. 6H). Meanwhile, the light-evoked current was abolished by 5 μM NBQX (Fig. 6H–I), which indicates that VTA D1 neurons activate LS neurons via releasing glutamate. We then investigated the expression of *Drd1* mRNA in VTA neurons which project to the LS with retrograde tracing and FISH (Supplementary Fig. 7). RetroAAV2-mCherry viruses were injected into the LS (Supplementary Fig. 7A), and the colocalizations between mCherry signal, *Drd1* mRNA, and *Vglut2*/*Vgat*/*Th* signal were detected in VTA. About 24% (202 $Drd1^{+}$/839 $mCherry^{+}$ neurons from 3 mice) VTA neurons projecting to the LS express *Drd1* mRNA, and more than 90% (78 $Vglut2^{+}$/83 $Drd1^{+}$ neurons) VTA $mCherry^{+}$/ $Drd1^{+}$ neurons are $Vglut2^{+}$, but few $Vgat^{+}$ or Th^{+} (Supplementary Fig. 7B). Together, these results suggest that VTA D1 neurons mainly release glutamate to excite LS neurons.

We further explored the involvement of LS-projecting VTA D1 neurons in regulating anxiety-like behaviors with pharmacological methods (Fig. 6J). Since activation of VTA D1 neurons increased the activity of LS neurons, we focused on the involvement of glutamatergic receptors and D1 receptors in LS. After blocking LS NMDA and AMPA receptors with AP5 and NBQX by cannula microinjection, activating VTA D1 neurons still increased mouse locomotor activity in open-field test, but had no significant effect on the time spent at center region, the ratio between center and surround speeds in open-field test (Baseline: 1.536 ± 0.323; Opto: 1.232 ± 0.151. $n = 11$ mice, $p = 0.5771$, Wilcoxon matched-pairs signed rank test), and the time spent at open arms in EPM test (Fig. 6K). On the contrary, after blocking LS D1 receptors with SCH23390, optical activating VTA D1 neurons had no significant effect on mouse locomotor speed in open-field test, but still tended to increase the time spent at center region and the time spent at open arms in EPM test (Fig. 6L). However, after blocking glutamatergic receptors or D1 receptors in NAc or mPFC, activating VTA D1 neurons can still have anxiolytic effects (Supplementary Fig. 8). Taken together, these results suggest that glutamatergic projection from VTA D1 neurons to the LS is responsible for relieving anxiety-like behaviors.

DISCUSSION

In this study, we uncovered the significance of VTA local DA signal on mouse anxiety level in both male and female. We demonstrate that (1) Manipulating VTA D1 receptors bidirectionally regulate mouse anxiety-like behaviors; (2) D1 receptors are functionally expressed in VTA neurons, and activating/silencing VTA D1 neurons oppositely modulate anxiety-like behaviors; (3) Glutamatergic projection of VTA D1 neurons to LS, but not other limbic regions, alleviates anxiety-like behavior. These results suggest the anxiolytic effect of D1 receptor expression in VTA glutamate neurons.

Though previous study in rats did not observe obvious D1 immunoreactivity in the VTA [38], we verified the expression of D1 receptors in mouse VTA neurons using a combination of a sensitive mRNA detection method - FISH, confocal imaging, D1-Cre mouse line, and electrophysiological recording (Fig. 2). Different from the abundant *Drd2* mRNAs expression in VTA DA neurons, sparse *Drd1* mRNA puncta were observed in VTA neurons (Supplementary Fig. 2). Sparse transcription of G protein-coupled receptors is not unusual and can provide sufficient receptors for functional modulation [64]. Activating D1 receptors will up-regulate neuronal excitability via several ways [65]. Our results showed that both D1 agonist and endogenous DA release are sufficient to activate D1 receptors expressed in VTA neurons, elevating neuronal activity (Fig. 2). Optically activating VTA DA neurons at 10 Hz and 20 Hz, but not 5 Hz, preferentially excited VTA neurons, which is consistent with the relatively low affinity of D1 receptors to DA and the preferentially sensitive of D1 receptors to the phasic DA change [66].

DA release in several brain regions is reported to have anxiolytic effect via D1 receptor-mediated signal pathway [6, 9, 10, 26]. However, similar as observed in our study, activating VTA DA neurons has no significant effect on the anxiety-like behaviors or even promotes some anxiety phenotypes [4, 26]. D2 receptors are extensively expressed in the VTA DA neurons [31, 46], and local VTA DA release will activate D2 receptors as negative feedback to inhibit DA neurons [30]. In VTA, somatodendritic dopamine release is inferred to be involved in the corticosterone-induced anxiety-like behaviors via D2 receptors [32]. Though we found that directly bidirectional manipulation of VTA D1 receptors controls mouse anxiety-like behavior, the inhibition effect of D2 receptors may override the anxiolytic effect of activating D1 receptors via endogenous DA release. In spite of sparse *Drd1* expression in the VTA, reducing VTA D1 receptors in VTA neurons elevates mouse anxious state (Figs. 1 and 5). Together, D1 and D2 receptors, these two complementary components expressed in VTA neurons,

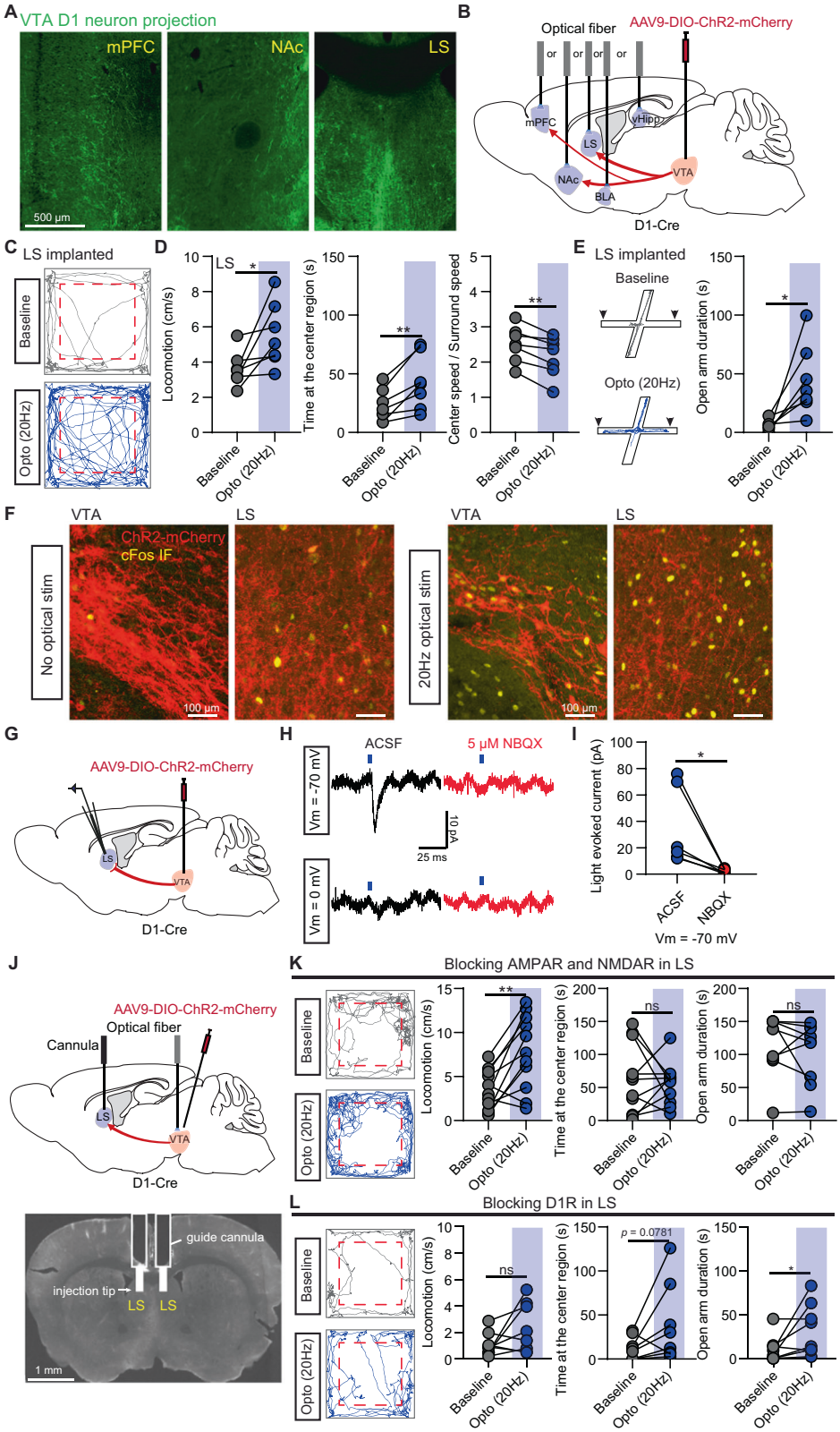

cooperate to control VTA neuronal excitability and balance the emotional behavior.

In brain, VTA neurons have diverse neural circuitry projections [67]. The well-studied downstream regions of VTA, such as mPFC, NAc, and vHipp, play vital roles in balancing emotional behaviors, and stimulating D1 neurons or D1 receptors in these regions has antidepressant and anxiolytic effects [6, 25, 68]. Our results show that activating VTA D1 neuronal axons in mPFC, NAc, vHipp, and amygdala has no effect on anxiety-like behaviors, but in LS exhibits anxiolytic effect (Fig. 6 and Supplementary Fig. 6). LS serves as an important relay center, which integrates cortical and subcortical inputs to regulate cognitive and emotional behaviors

Fig. 6 Glutamatergic projection of VTA D1 neurons to LS is responsible for alleviating mouse anxiety-like behaviors. A Example figures showing the distributions of VTA D1 neuronal axons labeled with eYFP viruses in mPFC (Left), NAc (Middle), and LS (Right). **B** Schematic of expressing ChR2-mCherry in VTA D1 neurons, followed with optical fiber implanted into mPFC, NAc, LS, BLA, or vHipp, respectively. **C** Example trajectories of one D1-Cre mouse in open-field test with optical fiber implanted into LS before (Top) and during (Bottom) light stimulation at 20 Hz. Dashed boxes indicate the center region. **D** Statistical results of activating VTA D1 neuronal axons in LS on mouse locomotor speed (Left), time spent at the center region (middle), and the ratio between locomotor speed at the center and surround regions (Right) in open-field test. $*p < 0.05$, $**p < 0.01$, Paired *t*-test, $n = 7$ (2 male and 5 female) mice. **E** Left: Example trajectories of one D1-Cre mouse in EPM test with optical fiber implanted into LS without (Top) and with (Bottom) light stimulation at 20 Hz. Arrows indicate the open arm side. Right: Statistical result of optogenetic activation of VTA D1 neuronal axons in LS on the duration spent at open arms in EPM test. $*p < 0.05$, Paired *t*-test, $n = 7$ (2 male and 5 female) mice. **F** Effects of optical activation of VTA D1 neurons at 20 Hz on the cFos expression (yellow) in VTA (Left) and LS (Right). **G** Schematic of viral transduction strategy using AAV9-DIO-ChR2-mCherry to express ChR2 in VTA D1 neurons and conduct whole-cell patch-clamp recording in the LS. **H** Example recording traces of one LS neuron in response to a 2-ms blue light stimulation when membrane voltage was held at −70 mV (Top) and 0 mV (Bottom) with normal ACSF (Baseline) and AMPA receptor blocker (NBQX). **I** Summary of optical evoked response amplitude when membrane voltage was held at −70 mV before and after applying NBQX. $*p < 0.05$, Wilcoxon matched-pairs signed rank test, $n = 6$ neurons from 4 mice. **J** Top: A diagram illustrating the locations of AAV-DIO-ChR2 virus injection, optical fiber implantation, and the cannulas used for local drug microinjection. Bottom: The example slice showing the location of cannulas. **K** Effect of blocking NMDA and AMPA receptors in LS when optical activation of VTA D1 neurons at 20 Hz. From left to right: Example trajectories in open-field test before and during activating VTA D1 neurons; statistical result of locomotor speed; statistical result of the time spent at the center region in open-field test; statistical result of the time spent at the open arms in EPM test. $n = 11$ (5 male and 6 female) mice for open-field test and 9 (4 male and 5 female) mice for EPM test, $**p < 0.01$, Wilcoxon matched-pairs signed rank test for open arm duration, and Paired *t*-test for the others. **L** Same as **K**, but for blocking D1 receptors with SCH23390 in LS. $n = 8$ female mice, $*p < 0.05$, Wilcoxon matched-pairs signed rank test.

[69–72]. The projection of VTA DA/glutamate neurons to LS has been reported [61, 63], but the possible functions of this neural circuit remain unclear. A recent study showed that VTA DA neurons projecting to LS promoted mouse aggression via D2 receptor-mediated inhibition of LS neurons [73]. Here, we uncover another role of VTA D1 neurons projecting to the LS in relieving anxiety-like behaviors via glutamatergic mechanism. Though activating LS type 2 CRF (CRFR2) neurons [69], oxytocin receptor neurons [71], and glutamatergic projection from mPFC to the LS increase anxiety-like behaviors [74], stimulation of the LS reduces feelings of fear and anxiety [72, 75]. Together with our study, we speculate that the diversity of LS neurons and their neural circuits may induce the oppositely anxiolytic and anxiogenic effects, and the target of VTA D1 neurons in LS remains to be further investigated.

Several evidence in our study support that the expression of D1 receptors in VTA glutamate neurons plays the dominant role in alleviating mouse anxiety-like behaviors. More than 40% *Drd1*$^+$ neurons in VTA are *Vglut2*$^+$, and ~20% VTA *Vglut2*$^+$ neurons express *Drd1* mRNA (Fig. 2). Meanwhile, activating VTA glutamate neurons, but not DA or GABA neurons, had an anxiolytic effect, and reducing D1 receptor expression in VTA glutamate neurons significantly elevated mouse anxious level (Fig. 5). More importantly, blocking glutamatergic synaptic transmission in LS, but not in NAc or mPFC, occluded the effect of activating VTA D1 neurons on mouse anxiety-like behaviors, and ~90% VTA *Drd1*$^+$ neurons projecting to the LS are *Vglut2*$^+$ (Fig. 6 and Supplementary Fig. 6). Similar as the VTA DA neurons, VTA glutamate neurons send axons to many brain regions and are involved in regulating multiple behaviors [46, 67]. VTA glutamate neurons are reported to regulate reward/aversion via projecting to NAc and lateral habenula [48, 58, 76–78], innate defensive behavior by receiving inputs from lateral hypothalamus [56], and wakefulness through projections to the NAc and the lateral hypothalamus [57]. A lot of studies suggest that VTA neurons projecting to different downstream targets have different anatomical locations or organizations, neuronal properties, input and output circuit architectures, and behavioral functions [60, 67, 79, 80]. Our study broadens the functional role and neural circuitry connection of VTA glutamate neurons in regulating emotional behaviors.

In this study, five different approaches were used to mutually investigate the roles of VTA D1 receptors/neurons in regulating anxiety-like behaviors. The anxiolytic effect of VTA D1 receptors/neurons is consistent, but some discrepancies between approaches were observed. Firstly, all the approaches, except for pharmacological manipulation, increased locomotor activity. Similar phenomena in locomotion as our study were also observed in mPFC and NAc [6, 81, 82]. Pharmacological manipulation would target all the D1 receptors expressed in neurons, non-neurons, and also afferent axons [83, 84], which may induce the different effects on locomotion from directly targeting neurons. Secondly, chemogenetic manipulation in open-field test, but not in EPM test, had significant anxiolytic effect. Mice in chemogenetic manipulation were used to run EPM test twice with the counter-balanced strategy, and repeated EPM test may cover the difference observed in other manipulation methods due to the familiar of EPM apparatus environment [51]. Thirdly, the TetTox approach decreased the time in open-field center but increased time in EPM open arms. TetTox is widely used to block neurotransmitters release, including GABA and glutamate, but DA release is resistant to the TetTox, which may due to lack machinery in DA neurons for TetTox uptake [54, 55]. TetTox may even elevate DA level [55], and knocking down D1 receptors in VTA DA neurons had prominent effect on EPM open arm durations, so TetTox may elevate brain DA to increase time in EPM open arms.

In conclusion, we uncovered the functional expression of D1 receptors in VTA neurons, and found the roles of VTA D1 receptors and D1 receptor expression neurons in regulating anxiety-like behaviors and identified the possible downstream brain region target. Activation of VTA D1 receptors obviously alleviates anxiety, which might serve as a potential target for anxiety disorder treatment.

REFERENCES

1. COVID-19 Mental Disorders Collaborators. Global prevalence and burden of depressive and anxiety disorders in 204 countries and territories in 2020 due to the COVID-19 pandemic. Lancet 2021;398:1700–12.
2. Tovote P, Fadok JP, Lüthi A. Neuronal circuits for fear and anxiety. Nat Rev Neurosci. 2015;16:317–31.
3. Zweifel LS, Fadok JP, Argilli E, Garelick MG, Jones GL, Dickerson TMK, et al. Activation of dopamine neurons is critical for aversive conditioning and prevention of generalized anxiety. Nat Neurosci. 2011;14:620–8.
4. Qi G, Zhang P, Li T, Li M, Zhang Q, He F, et al. NAc-VTA circuit underlies emotional stress-induced anxiety-like behavior in the three-chamber vicarious social defeat stress mouse model. Nat Commun. 2022;13:577.
5. Gunaydin LA, Grosenick L, Finkelstein JC, Kauvar IV, Fenno LE, Adhikari A, et al. Natural neural projection dynamics underlying social behavior. Cell 2014;157:1535–51.
6. Hare BD, Shinohara R, Liu RJ, Pothula S, DiLeone RJ, Duman RS. Optogenetic stimulation of medial prefrontal cortex Drd1 neurons produces rapid and long-lasting antidepressant effects. Nat Commun. 2019;10:223.

7. Chaudhury D, Walsh JJ, Friedman AK, Juarez B, Ku M, Koo JW, et al. Rapid regulation of depression-related behaviors by control of midbrain dopamine neurons. Nature 2013;493:532–6.
8. Friedman AK, Walsh JJ, Juarez B, Ku SM, Chaudhury D, Wang J, et al. Enhancing depression mechanisms in midbrain dopamine neurons achieves homeostatic resilience. Science 2014;344:313–9.
9. Xu XR, Xiao Q, Hong YC, Liu YH, Liu Y, Tu J. Activation of dopaminergic VTA inputs to the mPFC ameliorates chronic stress-induced breast tumor progression. CNS Neurosci Ther. 2021;27:206–19.
10. Nestler EJ, Carlezon WA. The mesolimbic dopamine reward circuit in depression. Biol Psychiatry. 2006;59:1151–9.
11. Liu J, Perez SM, Zhang W, Lodge DJ, Lu XY. Selective deletion of the leptin receptor in dopamine neurons produces anxiogenic-like behavior and increases dopaminergic activity in amygdala. Mol Psychiatry. 2011;16:1024–38.
12. Nguyen C, Mondoloni S, Le Borgne T, Centeno I, Come M, Jehl J, et al. Nicotine inhibits the VTA-to-amygdala dopamine pathway to promote anxiety. Neuron 2021;109:2604–15.e9.
13. Adell A, Artigas F. The somatodendritic release of dopamine in the ventral tegmental area and its regulation by afferent transmitter systems. Neurosci Biobehav Rev. 2004;28:415–31.
14. Rice ME, Patel JC. Somatodendritic dopamine release: recent mechanistic insights. Philos Trans R Soc B Biol Sci. 2015;370:20140185.
15. Missale C, Russel Nash S, Robinson SW, Jaber M, Caron MG. Dopamine receptors: from structure to function. Physiol Rev. 1998;78:189–225.
16. Nord M, Farde L. Antipsychotic occupancy of dopamine receptors in schizophrenia. CNS Neurosci Ther. 2011;17:97–103.
17. Ainsworth K, Smith SE, Zetterström TSC, Pei Q, Franklin M, Sharp T. Effect of antidepressant drugs on dopamine D1 and D2 receptor expression and dopamine release in the nucleus accumbens of the rat. Psychopharmacology 1998;140:470–7.
18. Hayden EP, Klein DN, Dougherty LR, Olino TM, Laptook RS, Dyson MW, et al. The dopamine D2 receptor gene and depressive and anxious symptoms in childhood: associations and evidence for gene-environment correlation and gene-environment interaction. Psychiatr Genet. 2010;20:304–10.
19. Lawford BR, Young R, Noble EP, Kann B, Ritchie T. The D2 dopamine receptor (DRD2) gene is associated with co-morbid depression, anxiety and social dysfunction in untreated veterans with post-traumatic stress disorder. Eur Psychiatry. 2006;21:180–5.
20. Zhang YQ, Lin WP, Huang LP, Zhao B, Zhang CC, Yin DM. Dopamine D2 receptor regulates cortical synaptic pruning in rodents. Nat Commun. 2021;12:6444.
21. Tu G, Ying L, Ye L, Zhao J, Liu N, Li J, et al. Dopamine D1 and D2 receptors differentially regulate Rac1 and Cdc42 signaling in the nucleus accumbens to modulate behavioral and structural plasticity after repeated methamphetamine treatment. Biol Psychiatry. 2019;86:820–35.
22. McNab F, Varrone A, Farde L, Jucaite A, Bystritsky P, Forssberg H, et al. Changes in cortical dopamine D1 receptor binding associated with cognitive training. Science 2009;323:800–2.
23. Goldman-Rakic PS, Castner SA, Svensson TH, Siever LJ, Williams GV. Targeting the dopamine D1 receptor in schizophrenia: Insights for cognitive dysfunction. Psychopharmacology 2004;174:3–16.
24. Hare BD, Duman RS. Prefrontal cortex circuits in depression and anxiety: contribution of discrete neuronal populations and target regions. Mol Psychiatry. 2020;25:2742–58.
25. Shuto T, Kuroiwa M, Sotogaku N, Kawahara Y, Oh YS, Jang JH, et al. Obligatory roles of dopamine D1 receptors in the dentate gyrus in antidepressant actions of a selective serotonin reuptake inhibitor, fluoxetine. Mol Psychiatry. 2020;25:1229–44.
26. DeGroot SR, Zhao-Shea R, Chung L, Klenowski PM, Sun F, Molas S, et al. Midbrain dopamine controls anxiety-like behavior by engaging unique interpeduncular nucleus microcircuitry. Biol Psychiatry. 2020;88:855–66.
27. Khlghatyan J, Quintana C, Parent M, Beaulieu J-M. High sensitivity mapping of cortical dopamine D2 receptor expressing neurons. Cereb Cortex. 2019;29:3813–27.
28. Paladini CA, Robinson S, Morikawa H, Williams JT, Palmiter RD. Dopamine controls the firing pattern of dopamine neurons via a network feedback mechanism. Proc Natl Acad Sci USA. 2003;100:2866–71.
29. Anzalone A, Lizardi-Ortiz JE, Ramos M, De Mei C, Hopf FW, Iaccarino C, et al. Dual control of dopamine synthesis and release by presynaptic and postsynaptic dopamine D2 receptors. J Neurosci. 2012;32:9023–34.
30. Ford CP. The role of D2-autoreceptors in regulating dopamine neuron activity and transmission. Neuroscience 2014;282:13–22.
31. De Jong JW, Roelofs TJM, Mol FMU, Hillen AEJ, Meijboom KE, Luijendijk MCM, et al. Reducing ventral tegmental dopamine D2 receptor expression selectively boosts incentive motivation. Neuropsychopharmacology 2015;40:2085–95.
32. Peng B, Xu Q, Liu J, Guo S, Borgland SL, Liu S. Corticosterone attenuates reward-seeking behavior and increases anxiety via D2 receptor signaling in ventral tegmental area dopamine neurons. J Neurosci. 2021;41:1566–81.
33. Schilström B, Yaka R, Argilli E, Suvarna N, Schumann J, Chen BT, et al. Cocaine enhances NMDA receptor-mediated currents in ventral tegmental area cells via dopamine D5 receptor-dependent redistribution of NMDA receptors. J Neurosci. 2006;26:8549–58.
34. Langlois LD, Dacher M, Nugent FS. Dopamine receptor activation is required for GABAergic spike timing-dependent plasticity in response to complex spike pairing in the ventral tegmental area. Front Synaptic Neurosci. 2018;10:32.
35. Ranaldi R, Wise RA. Blockade of D1 dopamine receptors in the ventral tegmental area decreases cocaine reward: possible role for dendritically released dopamine. J Neurosci. 2001;21:5841–6.
36. Matini T, Haghparast A, Rezaee L, Salehi S, Tehranchi A, Haghparast A. Role of dopaminergic receptors within the ventral tegmental area in antinociception induced by chemical stimulation of the lateral hypothalamus in an animal model of orofacial pain. J Pain Res. 2020;13:1449–60.
37. Moradi M, Fatahi Z, Haghparast A. Blockade of D1-like dopamine receptors within the ventral tegmental area and nucleus accumbens attenuates antinociceptive responses induced by chemical stimulation of the lateral hypothalamus. Neurosci Lett. 2015;599:61–6.
38. Yung KKL, Bolam JP, Smith AD, Hersch SM, Ciliax BJ, Levey AI. Immunocytochemical localization of D1 and D2 dopamine receptors in the basal ganglia of the rat: light and electron microscopy. Neuroscience 1995;65:709–30.
39. Dawson TM, Gehlert DR, Tyler McCabe R, Barnett A, Wamsley JK. D-1 dopamine receptors in the rat brain: a quantitative autoradiographic analysis. J Neurosci. 1986;6:2352–65.
40. Tiberi M, Jarvie KR, Silvia C, Falardeau P, Gingrich JA, Godinot N, et al. Cloning, molecular characterization, and chromosomal assignment of a gene encoding a second D1 dopamine receptor subtype: Differential expression pattern in rat brain compared with the D1A receptor. Proc Natl Acad Sci USA. 1991;88:7491–5.
41. Higa KK, Young JW, Ji B, Nichols DE, Geyer MA, Zhou X. Striatal dopamine D1 receptor suppression impairs reward-associative learning. Behav Brain Res. 2017;323:100–10.
42. Ji B, Higa K, Soontornniyomkij V, Miyanohara A, Zhou X. A novel animal model for neuroinflammation and white matter degeneration. PeerJ. 2017;5:e3905.
43. Xiao L, Priest MF, Kozorovitskiy Y. Oxytocin functions as a spatiotemporal filter for excitatory synaptic inputs to VTA dopamine neurons. Elife 2018;7:e33892.
44. Xiao L, Priest MF, Nasenbeny J, Lu T, Kozorovitskiy Y. Biased oxytocinergic modulation of midbrain dopamine systems. Neuron 2017;95:368–84.e5.
45. Chen S, Xu H, Dong S, Xiao L. Morpho-electric properties and diversity of oxytocin neurons in paraventricular nucleus of hypothalamus in female and male mice. J Neurosci. 2022;42:2885–904.
46. Morales M, Margolis EB. Ventral tegmental area: cellular heterogeneity, connectivity and behaviour. Nat Rev Neurosci. 2017;18:73–85.
47. Trudeau LE, Hnasko TS, Wallén-Mackenzie Å, Morales M, Rayport S, Sulzer D. The multilingual nature of dopamine neurons. Prog Brain Res. 2014;211:141–64.
48. Zell V, Steinkellner T, Hollon NG, Jin X, Zweifel LS, Hnasko TS, et al. VTA glutamate neuron activity drives positive reinforcement absent dopamine co-release. Neuron 2020;107:864–873.e4.
49. Gong S, Doughty M, Harbaugh CR, Cummins A, Hatten ME, Heintz N, et al. Targeting Cre recombinase to specific neuron populations with bacterial artificial chromosome constructs. J Neurosci. 2007;27:9817–23.
50. Durcan MJ, Lister RG. Time course of ethanol's effects on locomotor activity, exploration and anxiety in mice. Psychopharmacology 1988;96:67–72.
51. Schrader AJ, Taylor RM, Lowery-Gionta EG, Moore NLT. Repeated elevated plus maze trials as a measure for tracking within-subjects behavioral performance in rats (*Rattus norvegicus*). PLoS ONE. 2018;13:e0207804.
52. Zhou M, Liu Z, Melin MD, Ng YH, Xu W, Südhof TC. A central amygdala to zona incerta projection is required for acquisition and remote recall of conditioned fear memory. Nat Neurosci. 2018;21:1515–9.
53. Bergquist F, Niazi HS, Nissbrandt H. Evidence for different exocytosis pathways in dendritic and terminal dopamine release in vivo. Brain Res. 2002;950:245–53.
54. Liu C, Kaeser PS. Mechanisms and regulation of dopamine release. Curr Opin Neurobiol. 2019;57:46–53.
55. Whitton PS, Britton P, Bowery NG. Tetanus toxin alters 5-hydroxytryptamine, dopamine, and their metabolites in rat hippocampus measured by in vivo microdialysis. Neurosci Lett. 1992;144:95–8.
56. Barbano MF, Wang HL, Zhang S, Miranda-Barrientos J, Estrin DJ, Figueroa-González A, et al. VTA glutamatergic neurons mediate innate defensive behaviors. Neuron 2020;107:368–82.e8.
57. Yu X, Li W, Ma Y, Tossell K, Harris JJ, Harding EC, et al. GABA and glutamate neurons in the VTA regulate sleep and wakefulness. Nat Neurosci. 2019;22:106–19.
58. Qi J, Zhang S, Wang H-L, Barker DJ, Miranda-Barrientos J, Morales M. VTA glutamatergic inputs to nucleus accumbens drive aversion by acting on GABAergic interneurons. Nat Neurosci. 2016;19:725–33.

59. Han Y, Xia G, He Y, He Y, Farias M, Xu Y, et al. A hindbrain dopaminergic neural circuit prevents weight gain by reinforcing food satiation. Sci Adv. 2021;7:eabf8719.
60. Beier KT, Steinberg EE, DeLoach KE, Xie S, Miyamichi K, Schwarz L, et al. Circuit architecture of VTA dopamine neurons revealed by systematic input-output mapping. Cell 2015;162:622–34.
61. Khan S, Stott SRW, Chabrat A, Truckenbrodt AM, Spencer-Dene B, Nave KA, et al. Survival of a novel subset of midbrain dopaminergic neurons projecting to the lateral septum is dependent on neurod proteins. J Neurosci. 2017;37:2305–16.
62. Lammel S, Lim BK, Ran C, Huang KW, Betley MJ, Tye KM, et al. Input-specific control of reward and aversion in the ventral tegmental area. Nature 2012; 491:212–7.
63. Poulin J, Caronia G, Hofer C, Cui Q, Helm B, Awatramani R. Mapping projections of molecularly defined dopamine neuron subtypes using intersectional genetic approaches. Nat Neurosci. 2018;21:1260–71.
64. Guo Y, Xiao P, Lei S, Deng F, Xiao GG, Liu Y, et al. How is mRNA expression predictive for protein expression? A correlation study on human circulating monocytes. Acta Biochim Biophys Sin. 2008;40:426–36.
65. Surmeier DJ, Shen W, Day M, Gertler T, Chan S, Tian X, et al. The role of dopamine in modulating the structure and function of striatal circuits. Prog Brain Res. 2010;183:148–67.
66. Keeler JF, Pretsell DO, Robbins TW. Functional implications of dopamine D1 vs. D2 receptors: a 'prepare and select' model of the striatal direct vs. indirect pathways. Neuroscience 2014;282:156–75.
67. Beier KT, Gao XJ, Xie S, DeLoach KE, Malenka RC, Luo L. Topological organization of ventral tegmental area connectivity revealed by viral-genetic dissection of input-output relations. Cell Rep. 2019;26:159–67.e6.
68. Radke AK, Gewirtz JC. Increased dopamine receptor activity in the nucleus accumbens shell ameliorates anxiety during drug withdrawal. Neuropsychopharmacology 2012;37:2405–15.
69. Anthony TE, Dee N, Bernard A, Lerchner W, Heintz N, Anderson DJ. Control of stress-induced persistent anxiety by an extra-amygdala septohypothalamic circuit. Cell 2014;156:522–36.
70. Parfitt GM, Nguyen R, Bang JY, Aqrabawi AJ, Tran MM, Seo DK, et al. Bidirectional control of anxiety-related behaviors in mice: role of inputs arising from the ventral hippocampus to the lateral septum and medial prefrontal cortex. Neuropsychopharmacology 2017;42:1715–28.
71. Huang T, Guan F, Licinio J, Wong ML, Yang Y. Activation of septal OXTr neurons induces anxiety- but not depressive-like behaviors. Mol Psychiatry. 2021;26: 7270–9.
72. Wirtshafter HS, Wilson MA. Lateral septum as a nexus for mood, motivation, and movement. Neurosci Biobehav Rev. 2021;126:544–59.
73. Mahadevia D, Saha R, Manganaro A, Morgan AA, Dumitriu D, Rayport S, et al. Dopamine promotes aggression in mice via ventral tegmental area to lateral septum projections. Nat Commun. 2021;12:6796.
74. Chen Y, Yang J, Gao T, Chen Y, Wu J, Hu N, et al. Distinct projections from the infralimbic cortex exert opposing effects in modulating anxiety and fear Distinct projections from the infralimbic cortex exert opposing effects in modulating anxiety and fear. J Clin Investig. 2021;131:e145692.
75. Sheehan TP, Chambers RA, Russell DS. Regulation of affect by the lateral septum: Implications for neuropsychiatry. Brain Res Rev. 2004;46:71–117.
76. Root DH, Mejias-Aponte CA, Qi J, Morales M. Role of glutamatergic projections from ventral tegmental area to lateral Habenula in aversive conditioning. J Neurosci. 2014;34:13906–10.
77. Wang HL, Qi J, Zhang S, Wang H, Morales M. Rewarding effects of optical stimulation of ventral tegmental area glutamatergic neurons. J Neurosci. 2015;35: 15948–54.
78. Montardy Q, Zhou Z, Lei Z, Liu X, Zeng P, Chen C, et al. Characterization of glutamatergic VTA neural population responses to aversive and rewarding conditioning in freely-moving mice. Sci Bull. 2019;64:1167–78.
79. Lammel S, Ion DI, Roeper J, Malenka RC. Projection-specific modulation of dopamine neuron synapses by aversive and rewarding stimuli. Neuron 2011; 70:855–62.
80. de Jong JW, Afjei SA, Pollak Dorocic I, Peck JR, Liu C, Kim CK, et al. A neural circuit mechanism for encoding aversive stimuli in the mesolimbic dopamine system. Neuron. 2019;101:133–51.e7.
81. Zhu X, Ottenheimer D, DiLeone RJ. Activity of D1/2 receptor expressing neurons in the nucleus accumbens regulates running, locomotion, and food intake. Front Behav Neurosci. 2016;10:66.
82. Jang JK, Kim WY, Cho BR, Lee JW, Kim JH. Locomotor sensitization is expressed by ghrelin and D1 dopamine receptor agonist in the nucleus accumbens core in amphetamine pre-exposed rat. Addict Biol. 2018;23:849–56.
83. Kalivas PW, Duffy P. D1 receptors modulate glutamate transmission in the ventral tegmental area. J Neurosci. 1995;15:5379–88.
84. Nagatomo K, Suga S, Saitoh M, Kogawa M, Kobayashi K, Yamamoto Y, et al. Dopamine D1 receptor immunoreactivity on fine processes of GFAP-positive astrocytes in the substantia nigra pars reticulata of adult mouse. Front Neuroanat. 2017;11:3.

ACKNOWLEDGEMENTS

We thank Dr. Ping Zheng for D1-Cre mice, Dr. Xiaohong Xu for DAT-Cre mice, Dr. Miao He for Vgat-Cre and Vglut2-Cre mice, and the members of Xiao laboratory for their valuable input. We thank Dr. Lan Ma, Dr. Yevgenia Kozorovitskiy, Dr. Xin Jin, Dr. Qingjian Han, and Dr. Ting Lu for feedback on this manuscript. This work was supported by grants from the National Natural Science Foundation of China (81970727, 31900738, 31970908), Shanghai Municipal Science and Technology Major Project (No. 2018SHZDZX01), ZJ Lab, and Shanghai Center for Brain Science and Brain-Inspired Technology.

AUTHOR CONTRIBUTIONS

LX designed and supervised the study. QT and LX planned the experiments and analyzed the data. QT, XC, and XZ performed the behavioral experiments. QT and XC carried out FISH experiments. LX, HX, and SH carried out the electrophysiology experiments. QT, FH, and LX wrote the manuscript, and all of the authors helped with the revision of the manuscript.

COMPETING INTERESTS

The authors declare no competing interests.

ADDITIONAL INFORMATION

Supplementary information The online version contains supplementary material available at https://doi.org/10.1038/s41380-022-01809-y.

Correspondence and requests for materials should be addressed to Lei Xiao.

Reprints and permission information is available at http://www.nature.com/reprints

Publisher's note Springer Nature remains neutral with regard to jurisdictional claims in published maps and institutional affiliations.